© 2021. Published by The Company of Biologists Ltd | Journal of Cell Science (2021) 134, jcs259484. doi:10.1242/jcs.259484

RETRACTION

Retraction: Identification and characterization of GRIM-1, a cell-death-associated gene product

Edward R. Hofmann, Shreeram C. Nallar, Limei Lin, Jonathan D'Cunha, Daniel J. Lindner, Xiao Weihua and Dhananjaya V. Kalvakolanu

The journal has retracted *J. Cell Sci.* (2010) **123**, 2781-2791 (doi:10.1242/jcs.070250) in agreement with the authors.

Concerns were raised about duplications in the western blots shown in Fig. 5C and Fig. 5G. As the authors no longer have the original full blots, they cannot explain how these errors arose. Senior author, Dhananjaya Kalvakolanu, said, 'To be fair to the scientific community and prevent further propagation of these data, it is best to withdraw this paper from the public domain'.

Jonathan D'Cunha could not be contacted, but all other authors agree with this retraction.

Identification and characterization of GRIM-1, a cell-death-associated gene product

Edward R. Hofmann[1,*], Shreeram C. Nallar[1], Limei Lin[1], Jonathan D'Cunha[1], Daniel [illegible] Lindner[2], Jiao Weihua[3] and Dhananjaya V. Kalvakolanu[1,‡]

[1]Greenebaum Cancer Center, Department of Microbiology and Immunology, Molecular and Cellular Cancer Biology Track, GPILS, University of Maryland School of Medicine, Baltimore, MD 21201, USA
[2]Taussig Cancer Center, Lerner Research Institute, Cleveland, OH 44195, USA
[3]Hefei National Laboratory of Physical Sciences at Microscale, University of Science and Technology, Hefei, Anhui 230027, China
*Present address: Smith-Kline Beecham, Collegeville, PA 19426, USA
‡Author for correspondence (dkalvako@umaryland.edu)

Accepted 26 April 2010
Journal of Cell Science 123, 2781-2791

doi:10.1242/jcs.070250

Summary

Using a genome-wide technical knockout, we isolated a newly identified set of GRIM genes associated with retinoid-interferon-induced mortality) genes; GRIM genes mediate IFN- and retinoic-acid (RA)-induced cell death. Here, we describe the isolation and characterization of one such gene, *GRIM-1*. Three proteins, with identical termini, were produced from the *GRIM-1* open reading frame when this gene was transcribed and translated in vitro. These protein isoforms, designated GRIM-1α, GRIM-1β and GRIM-1γ, differentially suppressed growth via apoptosis in various cell lines. We also show that a caspase-dependent mechanism generates the proapoptotic GRIM-1 isoforms. Lastly, GRIM-1 isoforms differentially blocked maturation of 18S ribosomal RNA, consistent with their respective growth-suppressive ability. Together, these studies identified a novel protein involved in growth suppression and cell death.

Key words: Apoptosis, Cell growth, Cytokines

Introduction

Cytokines belonging to the interferon (IFN) group potentially suppress cell growth and promote apoptosis (Kimchi, 1992). They exert antiviral, immuno-regulatory and anti-proliferative effects employing the JAK (Janus tyrosine kinase)-STAT (signal transducer and activator of transcription) pathways (Stark and Darnell, 2007). Certain IFN-insensitive tumors become sensitive to IFNs when in the presence of all-*trans* retinoic acid (RA) (Moore et al., 1994). RA is a major physiological retinoid that binds to specific nuclear receptors (Chambon, 1996). The RA receptors act as transcription factors to drive expression of genes involved in cell differentiation and growth control. Retinoids inhibit growth of certain leukemias, skin dysplasias in vivo and tumor cell lines in vitro (Altucci and Gronemeyer, 2001). We have demonstrated earlier that the combination of both IFN and RA (IFN/RA) is a highly effective inhibitor of tumor growth in vivo and in vitro (Kalvakolanu, 2004; Lindner et al., 1997). Although IFN/RA combination induces apoptosis, the exact molecular mechanisms involved are still unclear.

Apoptosis eliminates superfluous and/or potentially dangerous cells in mammals. It is regulated by cytokines, survival factors, cell-cell and/or cell-ECM interactions, oncogenes, DNA damage and viral proteins (Ashkenazi and Dixit, 1998; Green and Reed, 1998; Stennicke and Salvesen, 2000; Youle and Strasser, 2008). Loss of apoptotic response seems to cause drug resistance in tumor cells (Ashkenazi and Dixit, 1998; Green and Reed, 1998; Logue and Martin, 2008; Lowe et al., 1994; Stennicke and Salvesen, 2000; Youle and Strasser, 2008). Although the roles of central players – such as caspases, Bcl2-like proteins and death receptors – in apoptotic responses have been well defined over the last decade, it is unclear how these proteins control cell death in a signal-specific and cell-type-specific manner. Via a positive-growth selection in the presence of cytotoxic agents, genome-wide expression-knockdown strategies permit the identification of gene products that are indispensable for cell-growth suppression or cell death. Such strategies do not require a prior knowledge about the gene(s) or their product(s) and allow an unbiased identification of activators of apoptosis (Deiss et al., 1995; Hofmann et al., 1998). We have employed one such approach, the antisense technical knockout (TKO), to isolate the GRIM (genes associated with retinoid-IFN-induced mortality) genes. In this approach, endogenous gene expression is knocked down by a library of antisense complementary DNAs (cDNAs) expressing from an episome. In this study, we have characterized a newly identified gene, *GRIM-1*, whose antisense expression protected cells from IFN/RA-induced cell death. The *GRIM-1* mRNA produces three protein isoforms, designated α, β and γ, from a single open reading frame (ORF); these isoforms induce cell death. Whereas GRIM-1γ can readily activate cell death, GRIM-1α and GRIM-1β required a proteolytic activation by caspase-9 to induce cell death. These isoforms suppress ribosomal RNA (rRNA) maturation to ablate cell growth. Together, these results identify a novel mediator and a novel cell-death-regulatory pathway.

Results

Identification of *GRIM-1* using a genetic approach

We isolated GRIM genes using the antisense TKO strategy (Angell et al., 2000; Hofmann et al., 1998). Briefly, HeLa cells were transfected with an antisense cDNA library and selected with hygromycin B (100 μg/ml) and a lethal dose of human IFNβ (5000 U/ml) and RA (5 μM) for 4 weeks. The surviving colonies were expanded and the episomal DNA bearing the death-associated gene

was isolated. One such episome carried an insert of 1.9 kb and was designated *GRIM-1*. Stable cell-line pools (n~150 colonies) were generated after transfecting pTKO1 or the same vector expressing antisense *GRIM-1* (pTKO1–GRIM-1) and selecting with hygromycin B. Upon exposure of the individual cells to IFN/RA for 4 weeks, the antisense-*GRIM-1*-episome-transfected but not the empty-vector-transfected cells formed viable colonies (Fig. 1A). Similar results were obtained with two other cell lines, MCF-7 and T47D (data not shown). In a separate experiment, equal numbers of pTKO1 cells and pTKO1–GRIM-1-expressing cells were seeded into 96-well plates, and were grown in the presence of a sub-lethal but growth-inhibitory concentration of human IFN-β (1000 U/ml) and RA (1 μM). In contrast to the pTKO1 cells, cells harboring pTKO1–GRIM-1 continued to grow in the presence of IFN/RA (Fig. 1B). Thus, antisense *GRIM-1* blocked IFN/RA-induced growth suppression and cell death.

To determine whether cell protection was indeed due to the production of antisense *GRIM-1* message, total RNA from the cells was subjected to a northern blot analysis with ^{32}P-labeled *GRIM-1* probe. In pTKO1 cells and pTKO1–GRIM-1-expressing cells, two *GRIM-1* RNAs, of ~2.7 and 3.0 kb, were detected. The basal expression of these RNAs was induced (~fivefold) upon IFN/RA treatment (Fig. 1C). These two RNAs correspond to endogenous *GRIM-1* transcripts. In pTKO1–GRIM-1-transfected cells, a new RNA band of 1.9 kb was present. This seems to be the antisense *GRIM-1* RNA, given its absence in the empty-vector-transfected cells. Because the antisense construct in the pTKO1 vector is under the control of an IFN-inducible promoter, antisense *GRIM-1* message was observed only in IFN/RA-treated cells. Consistent with these results, a loss of GRIM-1 protein expression occurred (see below). Thus, GRIM-1 seems to be a growth suppressor.

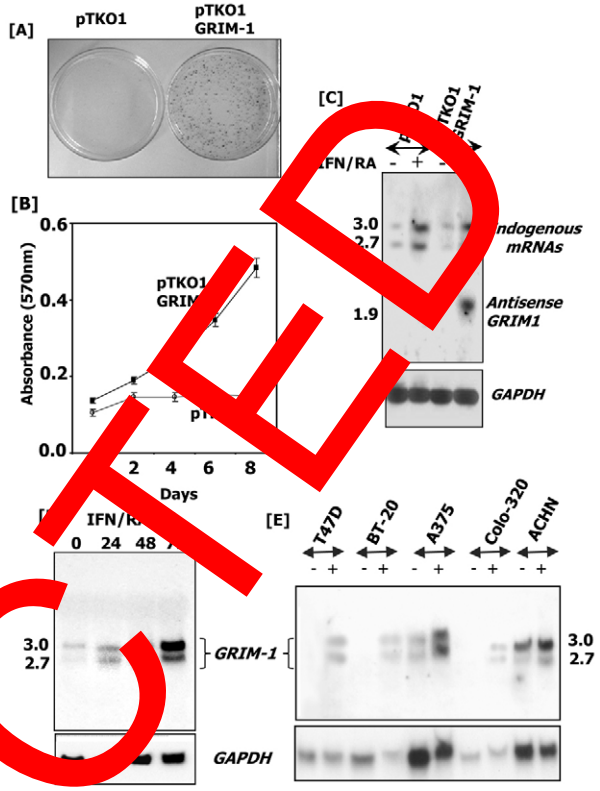

Fig. 1. *GRIM-1* is an IFN/RA-inducible gene that is essential for growth suppression mediated by IFN/RA. (**A**) HeLa cells transfected with pTKO1 or pTKO1–GRIM-1 and treated with IFN/RA for 4 weeks. Colonies are observed only in cells transfected with antisense *GRIM-1* (pTKO1–GRIM-1) because it confers a growth advantage to cells during IFN/RA treatment. (**B**) HeLa cells were stably transfected with pTKO1 or pTKO1–GRIM-1 and treated with IFN/RA for the indicated durations. A pool of 150 individual clones was used for this study. Growth assay was performed as mentioned in the Materials and Methods section. (**C**) Northern blot analysis of HeLa cells transfected with pTKO1 or pTKO1–GRIM-1 and treated with IFN/RA (+) for 48 hours were probed with ^{32}P-labeled *GRIM-1*-specific sequence (upper panel). Endogenous *GRIM-1* RNA (3.0 and 2.7 kb) levels are high following stimulation with IFN/RA compared with steady state (–). The 1.9-kb band represents antisense *GRIM-1* expressed from pTKO1. The blot was striped and reprobed with ^{32}P-labeled *GAPDH*-specific sequence (lower panel) to ensure comparable loading of RNA. (**D**) Northern blot analysis of *GRIM-1* induction in naive MCF-7 cells upon IFN/RA treatment. RNA prepared from MCF-7 cells at the indicated time points was probed with a ^{32}P-labeled *GRIM-1*-specific sequence (upper panel). The levels of *GRIM-1* RNA increase with time, indicative of transcriptional induction. The blot was striped and reprobed with ^{32}P-labeled *GAPDH*-specific sequence (lower panel) to ensure comparable loading of RNA. (**E**) *GRIM-1* is an IFN/RA-inducible gene in numerous cancer cell lines. Northern blot analysis of *GRIM-1* expression (upper panel) in the indicated cell lines treated with IFN/RA for 72 hours; *GAPDH* levels (lower panel) was used to access comparable loading of RNA. The cell lines are as follows: T47D and BT-20, estrogen-independent human breast carcinoma cell lines; A375, human melanoma; Colo-320, human colonic adenocarcinoma; ACHN, human renal cell carcinoma. Numbers adjacent to the blots indicate fragment size in kilobases.

IFN/RA induces *GRIM-1* RNA levels in multiple cell types

Because antisense *GRIM-1* expression conferred resistance to IFN/RA-induced death and two *GRIM-1* transcripts were detected in HeLa cells, we next examined the effects of IFN/RA on *GRIM-1* gene expression in the MCF-7 cell line. Initially, the course of IFN/RA response in MCF-7 cells was used to determine a suitable time point for analyzing *GRIM-1* expression. Total RNA from untreated and IFN/RA-treated cells was extracted and subjected to northern blot analysis with *GRIM-1* as probe. Similar to HeLa cells, MCF-7 cells also expressed two *GRIM-1* transcripts (sizes ~2.7 and 3.0 kb), the expressions of which were highly induced by IFN/RA (Fig. 1D). However, after 72 hours of exposure to IFN/RA, *GRIM-1* RNA levels declined (data not shown). This blot was subsequently hybridized to *GAPDH* probe (Fig. 1D) to ensure a comparable amount of RNA across lanes. This increase in *GRIM-1* transcripts also correlated with the time of significant cell death in these cell lines (data not shown). Consistent with these observations, northern blot analyses revealed two IFN/RA-inducible transcripts in five other cell lines (T47D, BT-20, A375, Colo-320 and ACHN) (Fig. 1E). In all cell lines, a higher steady-state level of *GRIM-1* was observed. In all cases, IFN/RA induced the expression of these RNAs, although the magnitude of induction was variable among these cell lines.

Analysis of *GRIM-1* cDNA

Because the antisense *GRIM-1* (1.9 kb) did not represent the full-length message(s), using a combination of cDNA-library screening and 5′RACE we cloned a cDNA of 2.7 kb, which corresponded to the smaller of the two RNAs detected in northern blots. Attempts to clone the 3.0-kb transcript were not successful. Sequence analysis of the 2.7-kb clone revealed the presence of a 1.7-kb ORF that encodes a 577-amino-acid polypeptide with a theoretical weight of 64.8 kDa. Database searches revealed that *GRIM-1* exhibited

homology to numerous human *SHQ1* entries (see supplementary material Table S1), although no protein(s) have been characterized to date. Despite its similarity with yeast Shq1p (Table 1), GRIM-1 exhibited a significant sequence divergence at its C-terminus. Thus, *GRIM-1* seems to be a distant ortholog of yeast *shq1*. Depletion of Shq1p in yeast causes severe growth retardation, owing to low ribosomal levels (Yang et al., 2002). A modular representation of GRIM-1 with putative domains (predictions made using Expasy, BLOCKS and MOTIF tools) is shown in Fig. 2A. Salient features are: (1) many leucine/isoleucine repeats that are six to eight amino acids apart are found between residues V358 and A438, indicating a potential leucine zipper-like motif; (2) a serine-rich C-terminus, suggesting potential regulation by serine/threonine kinases; and (3) actin crosslinking-like domain between residues S233 and P306. Other regions of interest are putative caspase-cleavage sites and multiple tyrosine residues that, if phosphorylated, could play an important role in the regulation of GRIM-1 function. A detailed characterization of the functional significance of these domains is underway.

The cloned human *GRIM-1* encodes three polypeptides

In order to ascertain whether *GRIM-1* actually encodes a protein, we performed coupled in vitro transcription and translation (Promega). The RNA from the full-length *GRIM-1* clone gave three polypeptides of 85, 75 and 45 kDa (Fig. 2B), much higher than the predicted weights of 65, 55 and 39 kDa, respectively. All three proteins were produced from a single ORF and the sizes of the proteins agreed with translation from three potential start sites located within the ORF. This was confirmed by cloning the three respective ORFs into pGEM-7zf and repeating the in vitro analysis (Fig. 2B). We have termed these three peptides as GRIM-1α, GRIM-1β and GRIM-1γ. Thus, *GRIM-1* mRNA can produce three proteins with identical C-termini in mammalian cells.

Multiple GRIM-1 peptides are induced by IFN/RA treatment

Because two *GRIM-1* transcripts were induced by IFN/RA (Fig. 2), we next determined whether the same was true at the protein level. A rabbit polyclonal IgG, raised against the C-terminal 203 amino acids of GRIM-1, was used in western blot analyses to determine the expression of GRIM-1 proteins in MCF-7 (Fig. 2C) and HeLa (data not shown) cells. In whole-cell extracts from both MCF-7 and HeLa cells, four to six bands ranging from 30 to 85 kDa were detected (Fig. 2C, upper panel), and all these proteins were induced upon IFN/RA treatment by 72 hours and continued to accumulate beyond 72 hours (data not shown). We arbitrarily named these bands α1, α2, β1, β2, γ1 and γ2 on the basis of their molecular sizes. The sizes of these bands were different from the predicted molecular weights of α, β or γ and their corresponding in vitro translated proteins, suggesting potential post-translational modification(s). The blot was stripped and reprobed with actin-specific antibody to ensure comparable protein loading (Fig. 2C).

To confirm the effect of antisense *GRIM-1* on these proteins, extracts from control and IFN/RA-treated (72 hours) HeLa cells carrying pTKO1 or pTKO1–GRIM-1 were subject to a western blot analysis. This experiment revealed that expression of the majority of GRIM-1-like polypeptides was knocked down in the presence of antisense *GRIM-1* (Fig. 2D, upper panel). This blot was stripped and re-probed with actin-specific antibody to ensure comparable protein loading (Fig. 2D, lower panel). Thus, the antisense-mediated knockdown of GRIM-1 proteins correlated with resistance to IFN/RA-mediated growth inhibition (see Fig. 1A,B).

Because the rabbit antibody produced a lot of background staining, it was not useful for in situ studies. To determine the location of endogenous GRIM-1, we analyzed cells by confocal microscopy using a mouse polyclonal GRIM-1-specific antibody. This antibody recognized the α, β and γ isoforms of GRIM-1, and yielded similar patterns to the rabbit polyclonal antibody in western blots (data not shown). GRIM-1-specific staining was observed in the cytoplasm and nucleus (Fig. 2E). To determine the effect of IFN/RA on GRIM-1, cells were treated with IFN/RA for 24 hours before processing. Upon IFN/RA treatment there was an increase in nuclear and cytoplasmic levels of GRIM-1 (Fig. 2E). In both cases, a focal staining was seen in the nuclei, indicating the association of GRIM-1 with sub-nuclear complexes and/or structures. The isotypic control IgG did not produce any signals in untreated or IFN/RA-treated cells (Fig. 2E). Because the antibody recognizes all GRIM-1 isoforms and isoform-specific reagents are not available at this stage, we employed epitope-tagged GRIM-1 constructs for determining their cellular localization. Cells were transfected with an empty vector (pCXN2) or individual Myc-tagged GRIM-1 isoforms. Cells were permeabilized, fixed and incubated with Myc-tag-specific antibody 24 hours post transfection. They were then incubated with an anti-mouse IgG labeled with Alexa Fluor 488. Like the native antibodies, the anti-Myc-tag antibody detected nuclear and cytoplasmic GRIM-1 staining. Interestingly, the GRIM-1γ-expressing cells had lobing of nuclei, which is an early sign of apoptosis. The empty-vector-transfected cells did not show any signals, indicating the specificity of detection (Fig. 2F). Although GRIM-1 was present in the cytoplasm diffusely, in the nucleus it localized primarily as distinct foci.

Overexpression of GRIM-1 isoforms sensitizes cells to IFN/RA-induced death

As mentioned earlier, antisense-mediated downregulation of GRIM-1 conferred resistance to IFN/RA-induced death (see Figs 1 and 2). Because three GRIM-1 peptides can be produced from a single RNA (see Fig. 2B), we next determined whether there

Table 1. Comparison of human GRIM-1 (577 aa) protein with other species

Species	Size (aa)	Identity	Similarity	Gaps
Pan troglodytes (Chimpanzee)	577	575/577 (99%)	575/577 (99%)	0/577 (0%)
Macaca mulatta (Monkey)	577	548/577 (94%)	561/577 (97%)	0/577 (0%)
Bos taurus (Cow)	579	460/581 (79%)	502/581 (86%)	6/581 (1%)
Mus musculus (Mouse)	569	423/570 (74%)	478/570 (83%)	13/570 (2%)
Rattus norvegicus (Rat)	603	432/606 (71%)	481/606 (79%)	44/606 (7%)
Caenorhabditis elegans	431	149/438 (34%)	227/438 (51%)	0/438 (6%)
Drosophila melanogaster	608	96/345 (27%)	156/345 (45%)	32/345 (9%)
Schizosaccharomyces pombe	451	155/445 (34%)	238/445 (53%)	33/445 (7%)
Saccharomyces cerevisiae	507	117/445 (26%)	212/445 (47%)	64/445 (14%)

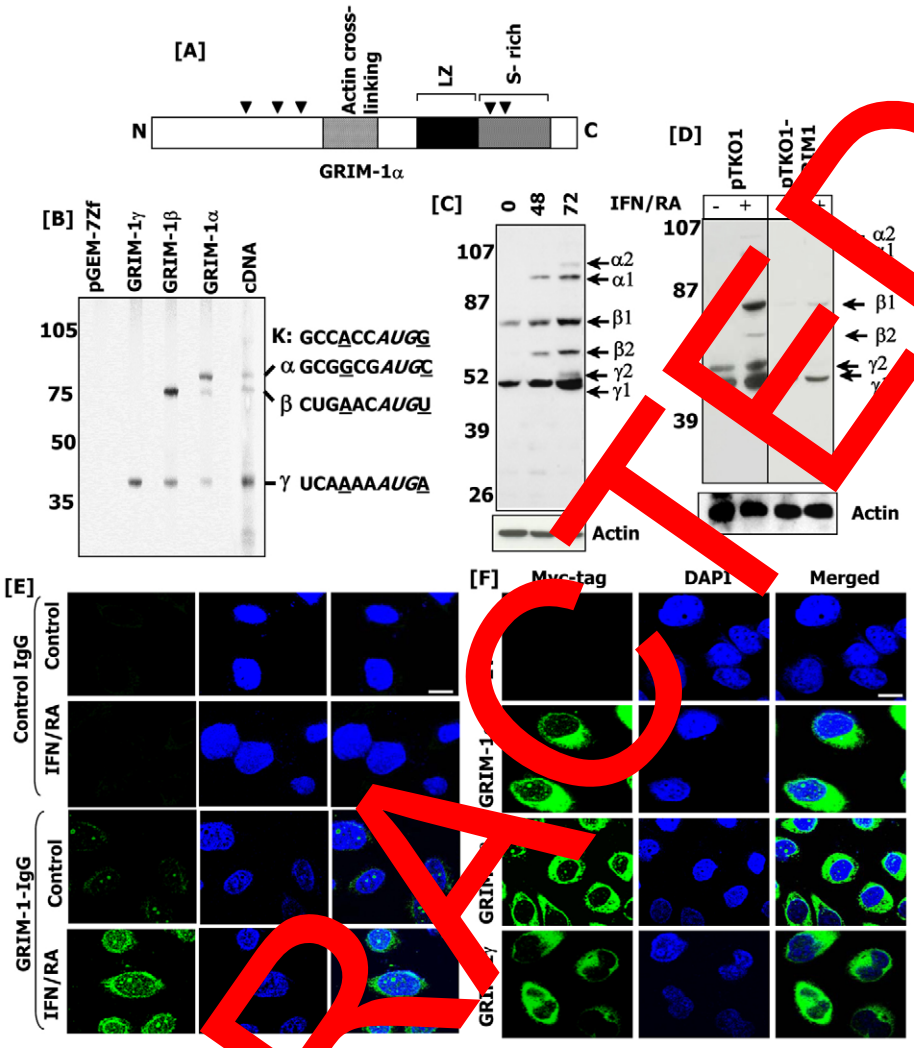

Fig. 2. Expression of GRIM-1 in cells. (**A**) Sch[illegible]atic repr[illegible]ation of putative domains and motifs in GRIM-1 protein. LZ, leucine zipper-like domain; S-rich, serine-rich region; arrowheads, putative caspa[illegible]cleavage sites; [illegible] terminus; C, C-terminus. (**B**) In vitro translation of *GRIM-1* ORFs resolved by SDS-PAGE. Lane marked as cDNA contained full-lengt[illegible]NA, whereas lanes ma[illegible] GRIM-1α, GRIM-1β and GRIM-1γ contained only putative ORFs of *GRIM-1*. pGEM-7Zf, empty cloning vector. Nucleotides a[illegible]ce[illegible] the putative translational start codon (*AUG*) are indicated on the right for all three ORFs and compared with an ideal Kozak sequence (K) required for[illegible]cient tra[illegible]on. (**C**) Western blot profile of GRIM-1 proteins in naive MCF-7 cells. Purified rabbit anti-GRIM-1 IgG was used. Hours of treatment are indicated above the bl[illegible]. (**D**) Western blot profile of GRIM-1 proteins in HeLa cells transfected with the indicated plasmids at steady state (–) and after 3 days of [illegible]/RA stimulation (+). [illegible] the appearance of distinctly sized proteins upon IFN/RA treatment in cells harboring empty vector (pTKO1), whereas the same ban[illegible]are markedly decreased in size for cells harboring antisense *GRIM-1* (pTKO1–GRIM-1). Numbers adjacent to the blots indicate the motilities of the molecular[illegible]ight mark[illegible] in kDa. (**E**) Cellular localization of GRIM-1 protein. Confocal images following incubation with a control IgG or a mouse polyclonal GRIM-1-[illegible]cific IgG. [illegible]F-7 cells were stained with DAPI to detect nuclei. GRIM-1 localizes as distinct foci in the nucleus. GRIM-1 levels are elevated upon IFN/RA trea[illegible]t and th[illegible]rotein accu[illegible]lates more in the cytoplasm, compared with control. (**F**) Cellular localization of GRIM-1 isoforms. pCXN2 vector (EV; empty vector) or th[illegible]ector expr[illegible]ng C-terminally Myc-epitope-tagged GRIM-1 isoforms were electroporated into MCF-7 cells. Twenty-four hours later cells were fixed and incu[illegible]d with M[illegible]-epitope-tag-specific antibodies. They were then stained with DAPI and anti-mouse IgG-tagged with Alexa Fluor 488. Images [illegible]red using a[illegible]f[illegible] microscope.

were diffe[illegible]ces in th[illegible]death-inductive properties. MCF-7 cells were transfe[illegible]d to[illegible]press individual GRIM-1 isoforms as Myc-tagged proteins.[illegible]nificantly fewer stable GRIM-1α ($P<0.05$), GRIM-1β ($P<0.01$)[illegible]d GRIM-1γ ($P<0.01$) colonies formed, compared with the con[illegible]l-vector transfectant (Fig. 3A). Cells expressing moderate levels of GRIM-1 isoforms grew slower compared with control-vector-transfected cells (Fig. 3B). We next examined the sensitivity of GRIM-1-expressing cells to IFN/RA-induced apoptosis by using TRITC-labeled-annexin-V binding as a tool. Indeed, cells expressing GRIM-1 isoforms were hypersensitive to IFN/RA-induced apoptosis compared with those expressing the control vector alone (Fig. 3C). Importantly, a high baseline apoptosis occurred upon GRIM-1 overexpression compared with vector control. In all three experiments above, the growth-suppressive and/or apoptotic effects of GRIM-1 isoforms were in the order of γ>β>α. The finding that IFN/RA further enhances GRIM-1-dependent death suggested that post-translation modifications and/or activation of other pathways that control GRIM-1 activity might play a role in promoting cell death. We also determined the expression of GRIM-1 isoforms by a western

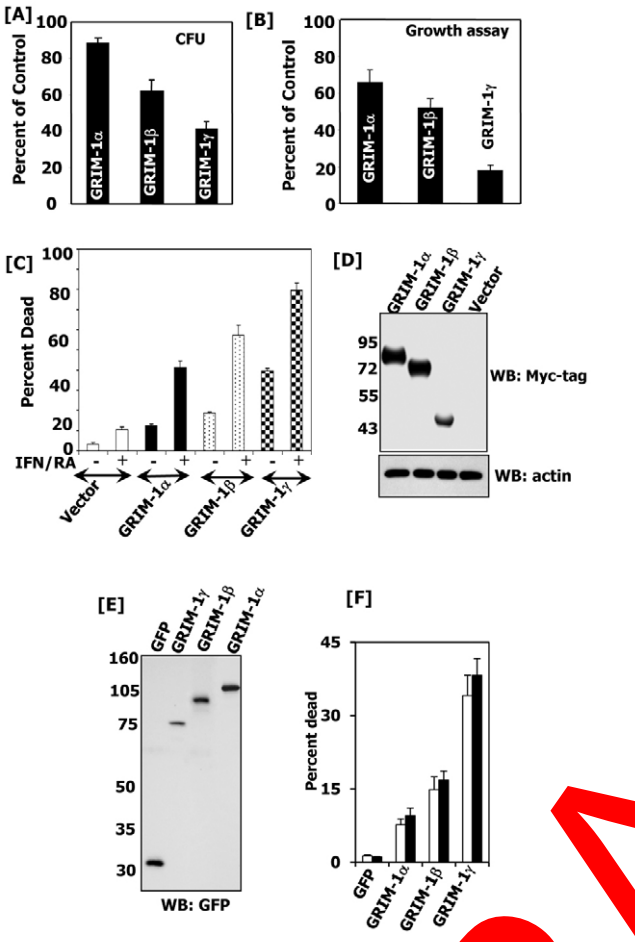

Fig. 3. GRIM-1 isoforms exert differential growth-suppressive potency. The indicated *GRIM-1* ORFs, expressed as C-terminal Myc-tagged proteins, transfected into MCF-7 cells were used to assess the effect of individual GRIM-1 isoforms on (A) colony formation, (B) growth and (C) sensitivity to IFN/RA treatment. (**A**) MCF-7 cells were transfected to express individual GRIM-1 isoforms. Twenty-four hours post transfection, cells were selected with G418 to kill non-transfected cells in the population. Cells were allowed to grow for 3 weeks before colony numbers were determined. (**B**) MCF-7 cells were manipulated as in A and cellular content, as a function of growth, was measured using a colorimetric assay. Only pools of colonies (~90) were used for these assays. (**C**) Expression of GRIM-1 isoforms sensitizes cells to IFN/RA treatment. MCF-7 cells were transfected with individual GRIM-1 isoforms. One set of cells was processed 24 hours post transfection (–) and another set was treated with IFN/RA (+) for 24 hours before processing. Cells were fixed, stained with TRITC-labeled annexin-V antibody and analyzed by FACS. (**D**) Western blot profiling the expression levels of Myc-tagged GRIM-1 isoforms (upper panel) in MCF-7 cells. Actin (lower panel) was used as a control for comparable protein loading. Numbers adjacent to the blots indicate the mobilities of the molecular-weight markers in kDa. (**E**) Western blot showing expression levels of GFP-tagged GRIM-1 isoforms. (**F**) Cell death induced by GRIM-1 isoforms. Cells were manipulated as in A and one set of cells were processed 24 hours post transfection for fluorescence microscopy (white bars) and another set was trypsinized and analyzed by FACS following incubation with TRITC-labeled annexin-V antibody (black bars). For microscopic analysis, GFP-positive cells from multiple (n=10) fields (~60 cells per field) were counted. GFP-positive cells with a rounded appearance and smaller nucleus (supplementary material Fig. S1) were counted as cells in the process of undergoing death (apoptosis). For FACS analysis, GFP-TRITC double-positive cells were counted as dead and expressed as a percentage of total GFP-positive cells (n=5/cell type) in this assay.

blot analysis of cellular lysates with a Myc-tag-specific antibody (Fig. 3D, upper panel). All three isoforms were expressed in MCF-7 cells. However, GRIM-1γ expressed at the lowest level compared with the others. The blot was stripped and re-probed with actin-specific antibody to ensure comparable protein loading (Fig. 3D, lower panel). We consistently observed a lower level of GRIM-1γ expression in other cell lines compared with GRIM-1α and GRIM-1β (data not shown). Although we have used annexin V as the marker for apoptosis, other characteristics such as caspase activation and nuclear fragmentation were noted in these cells (data not shown). However, MCF-7 cells do not undergo nuclear fragmentation owing to the lack of caspase-3 gene (Janicke et al., 1998).

Cellular sensitivity to GRIM-1-induced cell death was assessed using another transient assay. For this purpose, we infected HeLa cells with lentiviral particles encoding for GFP-tagged GRIM-1 isoforms. Twenty-four hours later, cells were fixed, stained with DAPI and observed using a fluorescent microscope, for dying cells. In initial studies we observed that cells expressing GFP–GRIM-1 isoforms round up overtime, unlike those expressing GFP alone (supplementary material Fig. S1). These cells also had fragmented and/or condensed nuclei, whereas no such changes were observed in control cells (supplementary material Fig. S2). We also ensured the expression of these constructs by performing a western blot analysis with a GFP-specific antibody (Fig. 3E); this corresponded to a shift towards higher molecular size. We counted green fluorescent cells from multiple independent fields with fragmented and/or condensed chromatin and expressed them as a percentage of total GFP-positive cells (Fig. 3F, white bars). The potency of GRIM-1 isoforms to induce cell death by this criterion was in the order of γ>β>α. This experiment was further supported by a FACS analysis of GFP–GRIM-1-expressing cells stained with TRITC-labeled annexin V. GFP and TRITC double-positive cells were calculated from total GFP-positive cells (Fig. 3F, black bars). The data obtained using these two methods were very similar. In summary, all three GRIM-1 isoforms induced apoptosis, with GRIM-1γ being the most potent.

Deletion of an N-terminal region in GRIM-1β enables it to drive GRIM-1γ-like cell death

Because GRIM-1α and GRIM-1β were weaker inducers of apoptosis compared with GRIM-1γ, we next checked whether there was an inhibitory region in these two proteins that prevents their spontaneous apoptotic activity. Given that GRIM-1α and GRIM-1β shared similar apoptotic properties and a common N-terminal region that is absent in GRIM-1γ, we generated serial N-terminal deletions to the GRIM-1β ORF (Fig. 4A) and cloned them downstream of the GFP tag in the pEGFP-C2 vector. We first ensured the expression of these deletion mutants. All chimeric proteins expressed with the expected sizes (Fig. 4B). The GRIM-1β deletions NΔ97 and NΔ121 expressed to a lower extent compared with GRIM-1β. Upon expression in MCF-7 cells, NΔ82, NΔ97 and NΔ121 robustly induced apoptosis, compared with the GRIM-1β and NΔ27 constructs (Fig. 4C). Similar results were obtained in HeLa and Cos-7 cells (data not shown). Thus, it seems that the proapoptotic activity of GRIM-1β is restrained by a domain located between amino acids 27 and 82 of its N-terminus. Interestingly, this region harbored potential caspase-cleavage sites. Therefore, in the next set of experiments, we examined the impact of caspase activities in stimulating the death-promoting activity of GRIM-1.

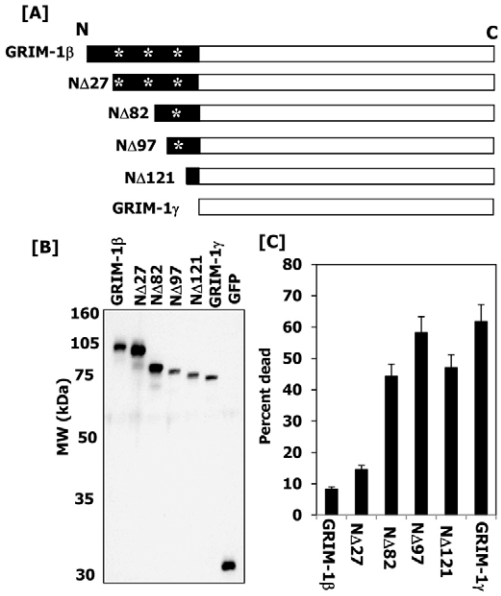

Fig. 4. The N-terminus of GRIM-1β harbors a death-inhibitory domain. (**A**) Modular representation of GRIM-1β deletions cloned in pEGFP-C2. The GFP tag is at the N-terminus of GRIM-1 isoforms. GRIM-1β and GRIM-1γ are shown for comparison. Putative caspase-cleavage sites (*) are indicated. (**B**) Western blot profile showing the expression of GFP-tagged GRIM-1β N-terminal deletions in MCF-7 cells. (**C**) MCF-7 cells were infected with lentiviral GFP-tagged GRIM-1β N-terminal-deletion constructs and cell death was quantified using annexin-V-stained samples on a FACS system. Double-positive cells (GFP and annexin V) were scored as dead.

GRIM-1α and GRIM-1β undergo a caspase-dependent processing

To determine the role of caspases in regulating GRIM-1 cleavage, we expressed GRIM-1α and GRIM-1β as N-terminal FLAG-tagged proteins (Fig. 5A), and then treated cells with IFN/RA. Fig. 5B shows a typical IFN/RA-induced cleavage of GRIM-1α and GRIM-1β proteins. IFN/RA treatment caused a decline of full-length protein level, which was accompanied by the appearance of a short N-terminal fragment that corresponds to the N-terminus. No such cleavage was observed in steady state. Because the N-terminal fragment, which bears the FLAG tag, is cleaved off, the larger processed GRIM-1 product could not be seen in these blots. In the next set of experiments we investigated whether Z-VAD-fmk, a pan-caspase inhibitor, could inhibit IFN/RA-induced cleavage of GRIM-1α and GRIM-1β. As controls, we used empty vector and FLAG–GRIM-1γ. Because there are no other cleavage products (see Fig. 5B), only the relevant portions of the blots in the experiments. As expected, in all cases no cleavage of GRIM-1α and GRIM-1β occurred in the untreated controls or in the presence of Z-VAD-fmk (Fig. 5C). However, IFN/RA treatment activated cleavage of GRIM-1α and GRIM-1β, which was inhibited in presence of Z-VAD-fmk. As expected, IFN/RA treatment did not induce the cleavage of GRIM-1γ. GRIM-1 cleavage occurred in a delayed manner, indicating the activation of additional processes, such as mitochondrial damage, prior to GRIM-1 activation.

Caspase-9 is important for the cleavage of GRIM-1α and GRIM-1β

Our previous studies indicated a role for caspases, in particular caspase-9, in the regulation of IFN/RA-induced cell death (Angell et al., 2000). Therefore, we next checked whether knockdown of caspase-9 affected IFN/RA-induced cleavage of GRIM-1α and GRIM-1β. Using specific lentiviral short hairpin RNAs (shRNAs), we knocked down the expression of caspase-9 in HeLa cells and measured its effects on IFN/RA-induced cleavage of GRIM-1α and GRIM-1β. The *CASP9*-specific shRNA knocked down >85% of endogenous protein compared with the controls (Fig. 5D, top panel). IFN/RA treatment activated a normal cleavage of GRIM-1α and GRIM-1β in the control cells but failed to do so in cells expressing *CASP9*-specific shRNA (Fig. 5D, middle panels). A comparable protein loading was confirmed by probing the blots with an actin-specific antibody (Fig. 5D, bottom panel). The importance of caspase-9 for the cleavage of GRIM-1α and GRIM-1β was further ascertained in a complementary experiment. *Casp9*$^{-/-}$ MEFs were transfected with expression vectors coding wild-type caspase-9 or a catalytically inactive mutant along with GRIM-1α or GRIM-1β. First, the expression of caspase-9 was confirmed by a western blot analysis (Fig. 5E, top panel). No IFN/RA-induced cleavage of GRIM-1α and GRIM-1β occurred in cells complemented with empty vector and/or mutant caspase-9 (Fig. 5E, middle panels). However, expression of wild-type caspase-9 complemented this defect and restored IFN/RA-induced cleavage of GRIM-1α and GRIM-1β. A comparable protein loading was ascertained by probing these blots with an actin-specific antibody (Fig. 5E, bottom panel). The above experiments indicated the involvement of mitochondrial damage in regulating the cleavage of GRIM-1. Therefore, we transfected GRIM-1β-expressing HeLa cells individually with expression vectors coding for Bcl2 (which blocks mitochondrial damage), Bax (which activates mitochondrial damage), wild-type caspase-9 or a catalytically inactive mutant and measured cell death. Cell death via GRIM-1β was robustly induced in the presence of Bax and caspase-9 (Fig. 5F, bars 3 and 4), whereas it was significantly lower in the presence of Bcl2 and mutant caspase-9 (Fig. 5F, bars 2 and 5). Similar results were obtained with GRIM-1α (data not shown). We also ensured the expression of the transfected Bcl2, Bax and caspase-9 by performing a western blot analysis of the extracts with specific antibodies. In all cases, corresponding protein bands were intense (compared with the controls) when the proteins were expressed (Fig. 5G). These results suggested that caspase-9 and mitochondrial damage are important for the induction of GRIM-1β and IFN/RA-driven apoptosis.

Because caspase activation seems to be a crucial step, we next examined whether mutation of potential caspase-cleavage sites would lead to suppression of GRIM-1β-induced apoptosis. On the basis of the observation that the NΔ97 mutant maximally induced cell death (see Fig. 4), similar to GRIM-1γ, and of the size of N-terminal protein generated by caspase cleavage (see Fig. 5), we decided to mutate the most probable caspase-cleavage site, located between positions 110 and 113, in the GRIM-1β protein: YLAD to YLAA. The effect of caspase-9 on the cleavage of the N-terminus of this mutant was determined by performing a western blot analysis with FLAG-tag-specific antibodies (Fig. 6A). Empty pCXN2 vector or the same vector carrying wild-type or mutant GRIM-1β were transfected along with wild-type caspase-9 into *Casp-9*$^{-/-}$ MEFs. As expected, wild-type GRIM-1β, but not the mutant GRIM-1β, was cleaved only in the presence of caspase-9.

Such a result was not due to a difference in expression levels of either mutant GRIM-1β or caspase-9. The incomplete cleavage might be due to low caspase activity in the transfectant, unlike under the conditions of IFN/RA treatment (see Fig. 5C), which unleashes many cooperative pathways. The negative control, empty-vector transfection, did not yield any signals, showing the specificity of detection.

To test the biological relevance of these observations, *Casp-9*$^{-/-}$ MEFs were transfected with wild-type and mutant GRIM-1β expression vectors in the absence and presence of caspase 9 (Fig. 6B). Although the magnitude of apoptosis was low in these MEFs, there were clear differences. A small but significant (P<0.05) apoptosis was observed upon transfection of either wild-type GRIM-1β or caspase-9; the level of apoptosis was synergistically induced when both proteins were present in the cells. Wild-type GRIM-1β potently induced apopto[illegible]sence of caspase-9 (P<0.01). Unlike wild type, the m[illegible]ant GRIM-1[illegible]iled to promote apoptosis. Thus, caspase-9 and [illegible]e YLAD site i[illegible]RIM-1β were required for promoting apopt[illegible] Consistent wi[illegible] these results, GRIM-1γ, which lacks these sites, [illegible]ivalently i[illegible]uced apoptosis in the absence and prese[illegible]e of caspas[illegible]in a [illegible]ntrol experiment (Fig. 6C).

GRIM-1 isoforms [illegible]terfere [illegible]th rRNA [illegible]aturation in vivo

As said earlier, GRIM[illegible] h[illegible]ologous [illegible]the yeast protein, Shq1p. Yeast mutants [illegible]pleted o[illegible]1p exhi[illegible] growth retardation owing to defects in [illegible]NA maturation[illegible]t al., 2002). Because GRIM-1 isoforms [illegible] to be potent growt[illegible] suppressors, we next examined their eff[illegible]s on [illegible]A processing. We used 18S RNA as a model for thes[illegible] experime[illegible] Total RNA purified from HeLa cells expressing Myc-tagged [illegible]M-1 isoforms was converted to cDNA usi[illegible]pecific primer in the invariant region of 18S rRNA. To [illegible]stinguish precursor versus mature 18S rRNA, we used primers [illegible]at overlapped [illegible] processed region and the invariant 18S region, [illegible]epresenting unp[illegible]essed and total rRNA, respectively, in PCR [illegible]g. 7A). In thes[illegible] reactions, a higher level of PCR signal, i.e. an ea[illegible] threshold [illegible]cle (C_t), with junction-specific primer(s) would be ind[illegible] of more unprocessed rRNA. Raw data from the junction-specific primer was normalized using the invariant primer [illegible]nd represented as the fraction of unprocessed rRNA. [illegible]xpression of GRIM-1 isoforms increased the fraction of 5′ETS (external transcribed spacer)-18S unprocessed rRNA (Fig. 7B). As observed earlier, a differential effect of GRIM-1 isoforms was noted in rRNA processing, with GRIM-1γ being the most potent

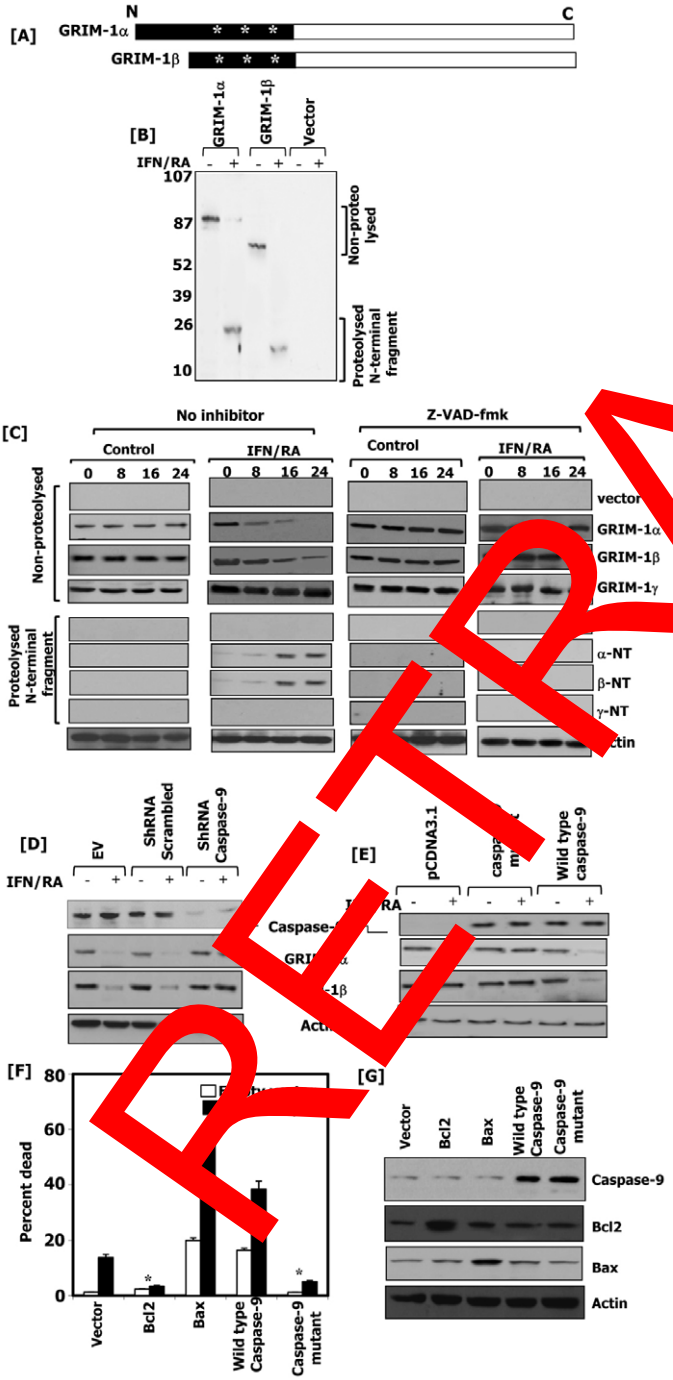

Fig. 5. IFN/RA-stimulated cleavage of GRIM-1α and GRIM-1β requires caspase-9. (**A**) Putative caspase-cleavage sites (*) in GRIM-1α and GRIM-1β are indicated. (**B**) Western blot profile of N-terminally FLAG-tagged GRIM-1 isoforms at steady state (–) and upon IFN/RA stimulation for 16 hours (+). The cleaved N-terminal region is seen as a fast-moving fragment. A FLAG-tag-specific antibody was used for detecting the products. (**C**) Western blot profile of HeLa cells expressing FLAG-tagged GRIM-1 isoforms stimulated with IFN/RA for the indicated time points in the absence and presence of pan-caspase inhibitor Z-VAD-fmk. A FLAG-tag-specific antibody was used for detecting the products and actin was used as a loading control. Isoforms 1α and 1β are cleaved but not 1γ. NT, N-terminal region. (**D**) Cleavage of GRIM-1 is absent upon expression of *CASP9*-specific shRNA. HeLa cells expressing *CASP9*-specific shRNA or a scrambled control shRNA or an empty vector (EV; pLKO1) were transfected with the indicated FLAG-tagged GRIM-1 isoforms. Cells were analyzed without (–) and with IFN/RA treatment for 24 hours (+) using caspase-9-specific and FLAG-tag-specific antibody. Presence of comparable protein loading was inferred using actin signals. (**E**) Caspase-9 is required for IFN/RA-stimulated cleavage of GRIM-1. *Casp9*$^{-/-}$ MEFs expressing the indicated FLAG-tagged GRIM-1 isoforms were transfected with the indicated caspase-9 expression constructs or empty vector (pCDNA3.1). Cells were analyzed without (–) and with IFN-β/RA treatment for 16 hours (+) using caspase-9-specific and FLAG-tag-specific antibody. Presence of comparable protein loading was inferred using actin signals. GRIM-1 isoforms are not cleaved upon expression of caspase-9 mutant or empty vector. (**F**) Loss of mitochondrial membrane potential is crucial for IFN/RA-induced cell death. HeLa cells expressing Myc-tagged GRIM-1β isoform were transfected with the indicated plasmids and cell death was measured. *, P<0.01. (**G**) Lysates from the indicated transfectants were employed for western blot analysis with the indicated antibodies on the right.

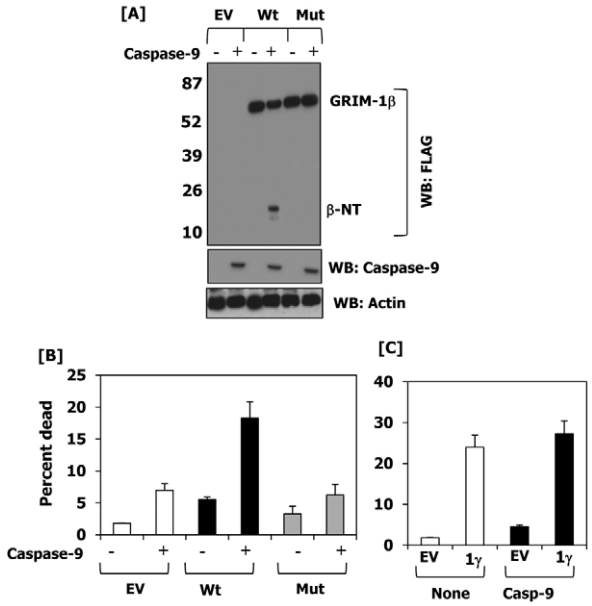

Fig. 6. Caspase-9-dependent activation of GRIM-1β and its ability to promote apoptosis are inhibited upon mutagenesis of the YLAD sequence. (**A**) FLAG-tagged wild-type and mutant GRIM-1β expression vectors were transfected into *Casp-9*$^{-/-}$ MEFs in the presence and absence of a vector coding for caspase-9. Cleavage of GRIM-1β was monitored as in Fig. 5. EV, empty vector (pCXN2); Wt, Wild-type GRIM-1β; Mut, YLAA-GRIM-1β. (**B**) Mutant GRIM-1β failed to promote caspase-9-dependent apoptosis. *Casp-9*$^{-/-}$ MEFs were transfected with the indicated expression vectors and apoptosis was monitored as in Fig. 5. (**C**) Empty vector (EV) and GRIM-1 (1γ) were transfected into *Casp-9*$^{-/-}$ MEFs, and apoptosis was monitored by annexin-V staining.

inhibitor of processing followed by GRIM-1β and G... compared with vector control. Thus, the grow... suppressive ability of GRIM-1 isoforms can be, in part, caused by ... pression of rRNA processing.

Suppression of tumor growth in vivo

Lastly, to determine the relevance of GRIM-1 to tumor growth, MCF-7 cells expressing individual Myc-tagged GRIM-1 isoforms

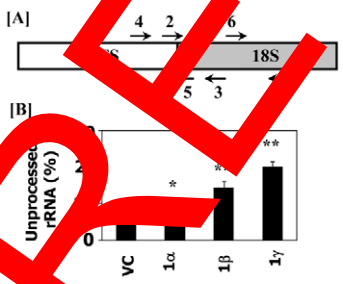

Fig. 7. GRIM-1 isoforms interfere with rRNA maturation. (**A**) Modular representation of 5′ETS-18S rRNA region showing relative primer positions (see supplementary material Table S2) used for analyzing rRNA processing following GRIM-1 expression. (**B**) Quantitative representation of unprocessed 18S rRNA relative to total 18S rRNA in HeLa cells expressing the indicated Myc-tagged GRIM-1 isoforms. *P* values: * <0.05 and ** <0.001 with respect to empty vector.

(see Fig. 3) were transplanted into athymic nude mice and tumor growth was monitored over a period of 12 weeks (Fig. 8A). The GRIM-1α, GRIM-1β and GRIM-1γ-expressing tumors grew significantly (the respective *P* values are <0.05, <0.01 and <0.005) slower than control tumors. At the end of 12 weeks, the average size of the control tumor was 12... mm^3. When compared with the control tumors, those expressing GRIM-1α, GRIM-1β or GRIM-1γ were significantly smaller, with mean tumor volumes of 95 mm^3 (*P*<0.05), 71 mm^3 (*P*<0.01) and 41 mm^3 (*P*<0.001), respectively. In a complementary experiment, we transplanted cells expressing empty vector (pTKO1) or antisense *GRIM-1* (see Fig. 1) into nude mice and tumor growth was monitored (Fig. 8B). Tumors expressing antisense *GRIM-1* grew significantly faster than those expressing empty vector (*P*<0.01). These differences in tumor growth were seen after 4 weeks and continued until the end of the study.

Discussion

Although the 'core' apoptotic machinery, consisting of the members of the BCL2 and caspase families, have been well characterized, it is still unclear how disparate exogenous and endogenous death stimuli control cell death in a signal- and cell-specific manner. In this report, we isolated a newly identified regulator of apoptosis, *GRIM-1*, using a genetic technique. The crucial role of GRIM-1 in mediating IFN/RA-induced cell death was highlighted by the following observations: (1) antisense expression of *GRIM-1* conferred resistance to IFN/RA-induced death (Fig. 1) and promoted tumor growth (Fig. 8B); and (2) its overexpression induced cell death (Figs 3, 4 and 5). We have found that IFN/RA was able to induce the expression of two *GRIM-1* transcripts in multiple cell types (Fig. 1). In HeLa cells, IFN-β alone induced expression of these mRNAs, but weaker than did IFN/RA, whereas RA had no effect on mRNA levels (data not shown). However, the fact that RA stimulated a similar mRNA (NCBI entry AK001401) in NT2 neuronal precursor cells, although the protein sequence differed at the N-terminus, was noteworthy.

GRIM-1 seems to be orthologous to *shq1* of *Saccharomyces cerevisiae* and *Schizosaccharomyces pombe*, and to other undefined proteins coded by *Drosophila melanogaster* and *Caenorhabditis*

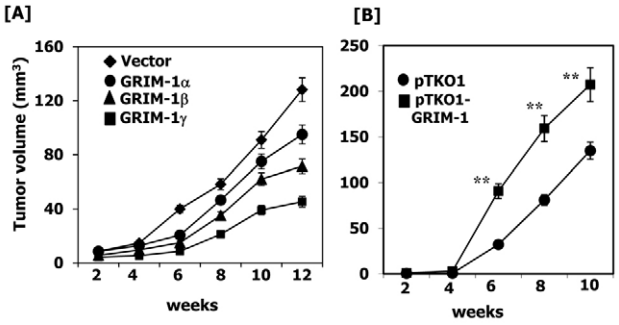

Fig. 8. Effect of GRIM-1 isoforms on tumor growth in vivo. (**A**) Athymic nude mice (*n*=7/group) were transplanted with MCF-7 cells (2×10^6) expressing individual GRIM-1 isoforms as in our earlier studies (Lindner et al., 1997). Tumor growth was measured over a period of 12 weeks. (**B**) Effect of GRIM-1 knockdown on tumor growth. MCF-7 cell lines expressing the indicated plasmids were transplanted into athymic nude mice (*n*=6/group) and tumor growth was monitored for 10 weeks. Statistical significance of the differences was obtained after comparing the tumor sizes to that of vector control in each case using Student's *t*-test. **P<0.01.

elegans (Table 1). The depletion of Shq1p in yeast causes growth retardation due to a defect in rRNA processing, thus highlighting its importance for cell growth (Yang et al., 2002). By contrast, we found that human GRIM-1 isoforms differentially suppress rRNA processing by acting as inhibitors (Fig. 7). The differential behavior of these two proteins could be due to intrinsic differences in their structure and/or regulation by other factors. These issues are currently being investigated.

Surprisingly, translation of a transcript derived from *GRIM-1* cDNA yielded three proteins in vitro (Fig. 2C). These observations are consistent with the expression of multiple proteins in cells as detected by the polyclonal antibodies (Fig. 2). Analysis of the DNA sequences around the putative start codons corresponding to GRIM-1 isoforms revealed the presence of a suboptimal Kozak sequences. Two crucial bases required for optimal initiation are the A in the –3 position and the G in the +4 position (Kozak, 1999). For GRIM-1α, neither the A–3 nor the G+4 were present (Fig. 2); although GRIM-1β and GRIM-1γ both have an A–3, neither have the G+4 base. Therefore, multiple GRIM-1 proteins observed in vivo can be produced either by translational control and/or by differential post-translational modification(s).

Cells expressing GRIM-1 isoforms grew significantly slower than the controls in vitro (Fig. 3) and in vivo (Fig. 8), thus highlighting their anti-tumor property. The anti-tumor activity in GRIM-1α- and GRIM-1β-expressing tumors might not be due to the production of GRIM-1γ as we did not observe a form consistent with GRIM-1γ in these tumors (data not shown). Such lack of expression of GRIM-1γ from *GRIM-1α* and *GRIM-1β* could also be due to the presence of an ideal Kozak sequence upstream of the translational start site and/or the 3′UTR of β-globin in these expression vectors, unlike the native mRNA. In summary, each of these proteins seems to exhibit differential anti-tumor properties. GRIM-1 seemed to activate apoptosis independently of other death regulators, such as p53, and this was supported by several observations. HeLa and Cos-7 cells lack endogenous p53 protein owing to degradation or physical binding by the viral proteins HPV-E6 and SV40 T-antigen, respectively (Finlay et al., 1989; Levine, 2009; Scheffner et al., 1990). Although MCF-7 cells possessed a wild-type p53, its inactivation by an overexpressed HPV-E6 did not substantially affect GRIM-1-driven apoptosis (data not shown). MCF-7 cells also lack caspase-3 owing to a genetic deletion (Janicke et al., 1998). On the basis of these observations, we propose that GRIM-1 induces apoptosis independently of p53 and caspase-3. Therefore, we investigated a mechanism of its activation.

Another mechanism that generates high levels of GRIM-1 isoforms in vivo occurs via a caspase-9-dependent conversion of high-molecular-weight forms of GRIM-1 to shorter death-activating forms in response to IFN/RA (Figs 5 and 6). An N-terminal sequence, present in GRIM-1α and GRIM-1β, seems to act as a negative regulator of its apoptotic activity. Deletion of the N-terminal sequences dramatically induced apoptosis (Fig. 4). It is possible that this domain folds back on to the C-terminus to prevent the apoptosis-inducing capacity of GRIM-1α and GRIM-1β. Indeed, it was recently shown that yeast Shq1p folds into two independent domains that contain sites of casein kinase 1 phosphorylation (Godin et al., 2009). Alternatively, it might associate with other undefined protein(s), which holds GRIM-1α or GRIM-1β in an inhibitory conformation. This region harbored three potential caspase-cleavage sites. It seems that one of the three potential cleavage sites present in this area, the third site (YLAD), is preferred for cleavage. Mutation of this site not only resulted in a failure to undergo caspase-9-dependent cleavage of GRIM-1β but also suppressed apoptosis (Fig. 6). Although it is theoretically possible for caspase-9 to play a role in GRIM-1γ-induced apoptosis, currently we do not have any data to that extent.

The role of caspases was based on our additional observations that, in the presence of Z-VAD-fmk and/or mutant caspase-9, cell death and IFN/RA-induced cleavage of GRIM-1α and GRIM-1β was blocked (Fig. 5). Consistent with these observations, Bcl2 blocked and Bax enhanced IFN/RA-induced and GRIM-1β-dependent apoptosis. Indeed, our earlier studies have shown caspase-9 activation and release of cytochrome *c* in response to IFN/RA (Angell et al., 2000; Ma et al., 2001). Caspases specifically cleave peptides after aspartic-acid residues (Nicholson and Thornberry, 1997). Recognition of at least four amino acids N-terminal to the site is also required. Several putative caspase-cleavage sites are present in GRIM-1 protein. Interestingly, many of the putative caspase-cleavage sites are conserved only in mammalian and *C. elegans* proteins, but not in yeast proteins. This is consistent with the fact that yeast does not have a known caspase (Wang et al., 1999). The presence of putative protein-interaction domains, phosphorylation sites and caspase-cleavage sites in the GRIM-1 protein suggests a highly ordered regulation of cell execution by GRIM-1, wherein several regulators converge on a single substrate. Indeed, deletion of an N-terminal region in GRIM-1β converted it into a GRIM-1γ-like death activator (Fig. 4). Activation of pro-death proteins via caspase-dependent cleavage is reported in other cases, e.g. death-promoting activity of mitochondrial regulator BID occurs via caspase-8-dependent cleavage (Li et al., 1998; Luo et al., 1998) and apoptotic activity of CAD, an endonuclease that fragments nuclear DNA, occurs via a caspase-3-dependent mechanism (Enari et al., 1998; Sakahira et al., 1998). Importantly, we have shown a newly identified IFN-inducible gene product that promotes IFN action by slowing rRNA maturation. However, a complete understanding of this regulation requires additional studies, which are currently being pursued.

We have previously reported that antisense-mediated inactivation of two other proteins, GRIM-12 (also known as TR; thioredoxin reductase) (Hofmann et al., 1998) and GRIM-19 (Angell et al., 2000), also suppressed cell death in response to IFN/RA. GRIM-12 was required for keeping the active sites of caspases in reduced state through its substrate thioredoxin (Ma et al., 2001). The second protein, GRIM-19, inhibits transcription factor STAT3 (Zhang et al., 2003), a protein known to upregulate the expression of mitochondrial antiapoptotic regulators Bcl2, Bcl-X_L and Mcl-1. It also represses the cell-death inducer FAS (Ivanov et al., 2001). We have shown that GRIM-19 antagonizes these functions of STAT3 to promote tumor suppression (Kalakonda et al., 2007). Indeed, we have recently documented loss of GRIM-19 in a number of primary tumors (Alchanati et al., 2006; Zhang et al., 2007). Loss of permeability of the mitochondrial membrane results in a release of apoptogenic proteins – including cytochrome *c* (Kluck et al., 1997; Liu et al., 1996), which is required for the activation of caspase-9. In our earlier studies, we have shown activation of caspase-9 (Angell et al., 2000; Ma et al., 2007) and cytochrome-*c* release in response to IFN/RA (Ma et al., 2001). In this study, we have shown that mutant caspase-9 and Bcl2 block the processing of GRIM-1. On the basis of our current data, we propose that GRIM-19 and GRIM-12 act upstream of GRIM-1 in the cell-death pathway regulated in response to IFN/RA treatment (Fig. 9). In summary,

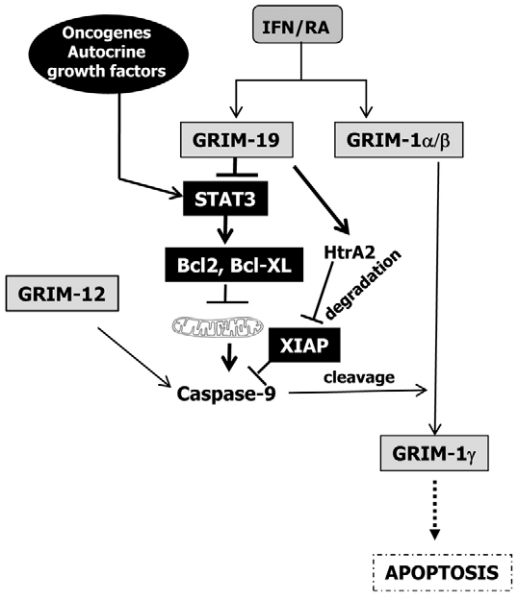

Fig. 9. A model for the anti-tumor actions of IFN/RA using GRIMs. All black and gray-colored objects represent growth-promoting and growth-suppressing factors, respectively. In tumor cells, oncogenic growth factors or activated oncogenes promote growth by upregulating anti-apoptotic factors, such as Bcl2 and Bcl-X_L. IFN/RA employs three GRIMs, GRIM-1, GRIM-12 and GRIM-19. Of these, GRIM-19 blocks STAT3, an oncogenic transcription factor (Zhang et al., 2003) to lower the levels of antiapoptotic factors. GRIM-19 also associates with a mitochondrial serine protease HtrA2 (Omi) to promote the degradation of XIAP (Ma et al., 2007), an inhibitor of caspases. Mitochondrial damage followed by apoptosome formation promotes the cleavage of GRIM-1. GRIM-12 activity maintains caspase-9 in an active state by providing the reducing power (Ma et al., 2001), promoting caspase-9 activity during IFN/RA treatment.

we identified a novel death-regulatory protein, whose activation by caspase-dependent mechanism(s) seems to contribute to apoptosis.

Materials and Methods

Reagents

Human IFNβ (Biogen), murine Ifnβ (R&D Systems), RA (Sigma), Z-VAD-fmk (Calbiochem), Ni-chelation sepharose (Novagen), ECL reagents (Pierce), HRP-coupled secondary antibodies (Amersham), hygromycin B (Boehringer Mannheim), DAPI (Sigma), and GFP-specific and caspase-9-specific antibodies (Santacruz Biotech) were employed in these studies. Lipofectamine-Plus (Invitrogen) was used for routine transfections as per the manufacturer's recommendation. Fresh stocks of RA were prepared in ethanol and added to cultures under subdued light.

Plasmids

Individual GRIM-1 isoforms were expressed as c-myc-tagged (at the C-terminus) proteins using pCX[illegible]-Myc vector (Hofmann et al., 1998), as FLAG-tagged (N-terminus) proteins from pCXN-FLAG vector and/or as GFP-tagged proteins using pEGFP-C2 (Clontech); expression vectors for wild-type and catalytically inactive caspase-9 were provided by [illegible] Srinivasula (NCI, Bethesda, MD), and Bax and Bcl2 were provided by Richard J. Youle (NIH-Bethesda, MD). To knock down endogenous GRIM-1, caspase-9, antisense *GRIM-1* in pTKO1 (Hofmann et al., 1998) and *CASP9*-specific shRNA in pLKO1 (Open Biosystems) were used, respectively. Lentiviral plasmids coding for GFP-tagged GRIM-1 isoforms were cloned into pLVX-Puro (Clontech) and shRNA constructs were produced as in our earlier publication (Gade et al., 2008). Deletion and site-directed mutagenesis, and northern and western blot analyses were performed as described earlier (Hofmann et al., 1998).

Cell culture

HeLa cells were cultured in DMEM containing 5% charcoal-stripped FBS, non-essential amino acids, L-glutamine and antibiotics. MCF-7 and T47D cell lines were cultured in Phenol-Red-free EMEM containing 5% charcoal-stripped FBS, non-essential amino acids, L-glutamine and 10^{-11} M estradiol during IFN/RA treatment. The BT-20 cell line was cultured in similar media with Phenol Red but supplemented with 5% charcoal-stripped FBS prior to IFN/RA treatment. Because Phenol Red in culture media exerts estrogenic effects, cells were grown in Phenol-Red-free media 24 hours before treatments were [illegible] *Casp9*$^{-/-}$ MEFs, provided by S. M. Srinivasula (NCI, Bethesda, MD) were grown in EMEM containing 5% FBS.

Cell growth assays

Cell growth was measured using a colorimetric assay (Skehan et al., 1990). Briefly, cells (2000 cells/well) were treated with human IFN-β (1000 U/ml) and RA (1 μM) in EMEM with 2.5% charcoal-stripped FBS in 96-well plates and fixed with 10% tri-chloro acetic acid (TCA) at the indicated time points. A control plate was fixed 8 hours after plating to determine the starting cell number. Plates were stained with 0.4% Sulforhodamine B (SRB; Sigma) prepared in 1% acetic acid for 1 hour; washed, dried and bound dye was extracted by adding 10 mM Tris-Cl (pH 10). The absorbance at 570 nm was quantified using a microplate reader.

Isolation of *GRIM-1*

A cDNA library was generated using poly(A)$^+$ RNA derived from the BT-20 cell line treated with human IFNβ (500 U/ml) and RA (1 μM) for 0, 2, 4, 8, 16, 24, 48 and 72 hours, pooled, converted to cDNA and inserted in antisense orientation and expressed from an episomal vector, pTKO1. This library was electroporated into cells and transfectants were selected with IFN/RA as described (Hofmann et al., 1998). The surviving colonies were expanded, and episomal DNA was extracted and transformed into *Escherichia coli* XL-10 to isolate the potential GRIM genes. Individual antisense GRIM genes were transfected into several cell lines to ensure protection against IFN/RA-induced apoptosis. One antisense clone identified in this manner contained a 2.1-kb fragment corresponding to the 3′ region of *GRIM-1* cDNA. This fragment was labeled with ^{32}P and used as a probe to screen a phage library. After three rounds of screening, two clones (~2.1 kb) were isolated. These clones, however, did not contain the 5′ end of the cDNA. Therefore, a 5′RACE was performed using a commercially available kit (Life Technologies). The RACE product was sequenced and then ligated to the 2.1-kb clone to generate the near-full-length cDNA (~2.7 kb).

In vitro transcription and translation

GRIM-1 cDNA and the indicated ORFs were subcloned into pGEM-7zf (Promega) under the control of T7 promoter. After linearizing the plasmid DNA (1 μg), with *Hin*dIII, it was programmed into rabbit reticulocyte lysate in a coupled in vitro transcription-translation system (Promega) in the presence of ^{35}S-methionine. The resultant products were separated by SDS-PAGE, dried and fluorographed.

Bacterial expression of GRIM-1 for polyclonal-antibody production

Initial attempts to express full-length *GRIM-1* ORF did not yield sufficient quantity of the protein. Hence, a cDNA fragment corresponding to the C-terminal 203 amino acids was cloned into pET-32b (Novagen) to generate the recombinant protein in *E. coli* BL21(DE3). Cells were lysed by sonication and GRIM-1 protein was purified from clarified supernatant using Ni-chelation Sepharose (Novagen) as recommended by the manufacturer. The purified GRIM-1 protein was digested with enterokinase, to remove the tag, and resolved by SDS-PAGE. The band corresponding to purified GRIM-1 peptide was used for antibody production in rabbits and mice.

Immunofluorescent and confocal microscopy

Cells cultured on cover glass in a 24-well tissue-culture plate were fixed for 15 minutes using 4% paraformaldehyde, permeabilized with 0.5% Triton X-100 in PBS and blocked in 5% BSA before additional processing. DAPI was used to visualize nuclei. Direct or indirect fluorescence was employed to visualize tagged GRIM-1 isoforms. Images were captured using a fluorescence microscope (Olympus BX-FLA, Osaka) fitted with a digital camera (QICAM), and processed by Q-capture Pro 5.1 (Q-Imaging Corporation) or using a confocal microscope (Zeiss LSM 510). Cell numbers were determined using immunofluorescent images from ten randomly selected fields, with each field containing ~60 cells and subjected to statistical analysis with Student's *t*-test.

Tumorigenic assays

Three- to four-week-old athymic nude (*nu/nu*) NCr mice (Taconic) were used in the study (Lindner et al., 1997). Procedures involving animals and their care were conducted in conformity with the institutional guidelines that comply with national and international laws and policies (EEC Council Directive 86/609, OJL 358, 1 Dec. 1987, and the National Institutes of Health Guide for the Care and Use of Laboratory Animals, NIH Publication No. 85-23, 1985). Cells (2×10^6) were injected into flanks in the mid-axillary line and tumor growth was monitored over a period of 12 weeks. Tumor volume (V) was calculated using caliper measurements and the formula: $V=(4/3)\pi a^2 b$, where $2a$ = minor axis, $2b$ = major axis of the prolate spheroid. Student's *t*-test was used to assess the statistical significance of difference between pairs of samples.

Reverse transcriptase PCR analysis of rRNA

Total RNA was converted to cDNA using an rRNA-specific primer (supplementary material Table S2). Unprocessed 5′ETS-18S and processed 18S rRNA fraction were obtained using specific primer pairs (supplementary material Table S2) as shown in Fig. 8. Unprocessed 5′ETS-18S rRNA was represented as fraction of total 18S rRNA pool using the Δ^{Ct} method (Nolan et al., 2006).

D.V.K. is supported by NIH grants CA105005 and CA78282. Deposited in PMC for release after 12 months.

Supplementary material available online at
http://jcs.biologists.org/cgi/content/full/123/16/2781/DC1

References

Alchanati, I., Nallar, S. C., Sun, P., Gao, L., Hu, J., Stein, A., Yakirevich, E., Konforty, D., Alroy, I., Zhao, X. et al. (2006). A proteomic analysis reveals the loss of expression of the cell death regulatory gene GRIM-19 in human renal cell carcinomas. *Oncogene* **25**, 7138-7147.

Altucci, L. and Gronemeyer, H. (2001). The promise of retinoids to fight against cancer. *Nat. Rev. Cancer* **1**, 181-193.

Angell, J. E., Lindner, D. J., Shapiro, P. S., Hofmann, E. R. and Kalvakolanu, D. V. (2000). Identification of GRIM-19, a novel cell death-regulatory gene induced by the interferon-beta and retinoic acid combination, using a genetic approach. *J. Biol. Chem.* **275**, 33416-33426.

Ashkenazi, A. and Dixit, V. M. (1998). Death receptors: signaling and modulation. *Science* **281**, 1305-1308.

Chambon, P. (1996). A decade of molecular biology of retinoic acid receptors. *FASEB J.* **10**, 940-954.

Deiss, L. P., Feinstein, E., Berissi, H., Cohen, O. and Kimchi, A. (1995). Identification of a novel serine/threonine kinase and a novel 15-kD protein as potential mediators of the gamma interferon-induced cell death. *Genes Dev.* **9**, 15-30.

Enari, M., Sakahira, H., Yokoyama, H., Okawa, K., Iwamatsu, A. and Nagata, S. (1998). A caspase-activated DNase that degrades DNA during apoptosis, and its inhibitor ICAD. *Nature* **391**, 43-50.

Finlay, C. A., Hinds, P. W. and Levine, A. J. (1989). The p53 proto-oncogene can act as a suppressor of transformation. *Cell* **57**, 1083-1093.

Gade, P., Roy, S. K., Li, H., Nallar, S. C. and Kalvakolanu, D. V. (2008). Cr[illegible] for transcription factor C/EBP-beta in regulating the expression of death-ass[illegible]ted protein kinase 1. *Mol. Cell. Biol.* **28**, 2528-2548.

Godin, K. S., Walbott, H., Leulliot, N., van Tilbeurgh, H. and Varani, G. (2009). [illegible] box H/ACA snoRNP assembly factor Shq1p is a chaperone protein homologous [illegible] Hsp90 cochaperones that binds to the Cbf5p enzyme. *J. Mol. Biol.* [illegible]231-244.

Green, D. R. and Reed, J. C. (1998). Mitochondria and apoptos[illegible] [illegible]81, 1309-1311.

Hofmann, E. R., Boyanapalli, M., Lindner, D. J., Weihua, X[illegible]assel, B. A[illegible]agus, R., Gutierrez, P. L. and Kalvakolanu, D. V. (1998). Thiore[illegible]n reductase death effects of the combination of beta interferon and re[illegible] acid. *Mo[illegible]ell. Biol.* **18**, 6493-6504.

Ivanov, V. N., Bhoumik, A., Krasilnikov, M., Raz, R[illegible]Owen-Sc[illegible]L. B., Levy, D., Horvath, C. M. and Ronai, Z. (2001). Coo[illegible]tion between [illegible]3 and c-jun suppresses Fas transcription. *Mol. Cell* **7**, 517-5[illegible]

Janicke, R. U., Sprengart, M. L., Wati, M. R[illegible]Porter, A. G. (1998). Ca[illegible]se-3 is required for DNA fragmentation and morph[illegible]gica[illegible]ges associated with apoptosis. *J. Biol. Chem.* **273**, 9357-9360.

Kalakonda, S., Nallar, S. C., Lindner, D. J., Hu, J., Reddy,[illegible]and Kalvakolanu, D. V. (2007). Tumor-suppressive activ[illegible] of the cell death ac[illegible] GRIM-19 on a constitutively active signal transduc[illegible]nd activator of transcription[illegible] *Cancer Res.* **67**, 6212-6220.

Kalvakolanu, D. V. (2004). The [illegible]MMs: a new[illegible]terface between cell death regulation and interferon/retinoid induc[illegible]rowth supp[illegible]ion. *Cytokine Growth Factor Rev.* **15**, 169-194.

Kang, J. J., Schaber, M. D., S[illegible]asula[illegible]M., Alnemri[illegible]S., Litwack, G., Hall, D. J. and Bjornsti, M. A. (1999). C[illegible]of mammali[illegible]aspase activation in the yeast Saccharomyces cerevisiae. *J. Biol. C[illegible]***274**, 3189[illegible]98.

Kimchi, A. (1992). Cytokine triggered molecular pathways that control cell cycle arrest. *J. Cell. Biochem.* **50**, 1-9.

Kluck, R. M., Bossy-Wetzel, E., Green, D. R. and Newmeyer, D. D. (1997). The release of cytochrome c from mitochondria: a primary site for Bcl-2 regulation of apoptosis. *Science* **275**, 1132-1136.

Kozak, M. (1999). Initiation of translation in prok[illegible]eukaryotes. *Gene* **234**, 187-208.

Levine, A. J. (2009). The common mecha[illegible]ns of transform[illegible] by the small DNA tumor viruses: The inactivation of tumo[illegible]ppressor gene produ[illegible]p53. *Virology* **384**, 285-293.

Li, H., Zhu, H., Xu, C. J. and Yuan, J. ([illegible]). Cleavage of BID b[illegible]aspase 8 mediates the mitochondrial damage in the Fas pathw[illegible]apoptosis. *Cell*[illegible], 491-501.

Lindner, D. J., Borden, E. C. a[illegible]Kalvakolani[illegible]V. (1997[illegible]ynergistic antitumor effects of a combination of in[illegible]erons and retinoic[illegible]n l[illegible]an tumor cells in vitro and in vivo. *Clin. Cancer R[illegible]***3**, 931-937.

Liu, X., Kim, C. N., Yan[illegible], Jemmer[illegible] R. and Wang, X. (1996). Induction of apoptotic program in c[illegible]ee extracts[illegible]quirement for dATP and cytochrome c. *Cell* **86**, 147-157.

Logue, S. E. and Martin, S.[illegible]2008[illegible]aspase activ[illegible]n cascades in apoptosis. *Biochem. Soc. Trans.* **36**, 1[illegible]

Lowe, S. W., Bod[illegible]S., McClatche[illegible]Remi[illegible]on, L., Ruley, H. E., Fisher, D. E., Housman, D[illegible]and Jacks, T. (199[illegible]tus and the efficacy of cancer therapy in vivo. *Sci*[illegible]**66**, 807-810.

Luo, X., Bu[illegible]ár[illegible]Zou, H., Slaughter, C. and Wang, X. (1998). Bid, a Bcl2 interacti[illegible]protein, [illegible]es cytochrome c release from mitochondria in response to activati[illegible]of cell surface[illegible]receptors. *Cell* **94**, 481-490.

Ma, X., Karra, S., Guo, W.,[illegible]er, D. J., Hu, J., Angell, J. E., Hofmann, E. R., Red[illegible]P. and Kalvakolanu,[illegible]V. (2001). Regulation of interferon and retinoic [illegible]induced cell death activation through thioredoxin reductase. *J. Biol. Chem.* **276**, 24843-24854.

[illegible]a, X., Kalakonda[illegible], Srinivasula, S. M., Reddy, S. P., Platanias, L. C. and Kalvakolanu, D. V.[illegible]007). GRIM-19 associates with the serine protease HtrA2 for promoting cell death[illegible]*ncogene* **26**, 4842-4849.

[illegible]ore, D. M., Kalva[illegible]anu, D. V., Lippman, S. M., Kavanagh, J. J., Hong, W. K., [illegible]rden, E. C., Pa[illegible]es-Espinoza, M. and Krakoff, I. H. (1994). Retinoic acid and i[illegible]on in hu[illegible]cancer: mechanistic and clinical studies. *Semin. Hematol.* **31**, 31-37.

Nicholson, D. W. and Thornberry, N. A. (1997). Caspases: killer proteases. *Trends [illegible]Biochem. Sci.* **22**, 299-306.

[illegible]nds, R. E. and Bustin, S. A. (2006). Quantification of mRNA using real-time RT-PCR. *Nat. Protoc.* **1**, 1559-1582.

Sakahira, H., Enari, M. and Nagata, S. (1998). Cleavage of CAD inhibitor in CAD activation and DNA degradation during apoptosis. *Nature* **391**, 96-99.

Scheffner, M., Werness, B. A., Huibregtse, J. M., Levine, A. J. and Howley, P. M. (1990). The E6 oncoprotein encoded by human papillomavirus types 16 and 18 promotes the degradation of p53. *Cell* **63**, 1129-1136.

[illegible]chindler, C., Levy, D. E. and Decker, T. (2007). JAK-STAT signaling: from interferons to cytokines. *J. Biol. Chem.* **282**, 20059-20063.

Skehan, P., Storeng, R., Scudiero, D., Monks, A., McMahon, J., Vistica, D., Warren, J. T., Bokesch, H., Kenney, S. and Boyd, M. R. (1990). New colorimetric cytotoxicity assay for anticancer-drug screening. *J. Natl. Cancer Inst.* **82**, 1107-1112.

Stennicke, H. R. and Salvesen, G. S. (2000). Caspases-controlling intracellular signals by protease zymogen activation. *Biochim. Biophys. Acta* **1477**, 299-306.

Yang, P. K., Rotondo, G., Porras, T., Legrain, P. and Chanfreau, G. (2002). The Shq1p.Naf1p complex is required for box H/ACA small nucleolar ribonucleoprotein particle biogenesis. *J. Biol. Chem.* **277**, 45235-45242.

Youle, R. J. and Strasser, A. (2008). The BCL-2 protein family: opposing activities that mediate cell death. *Nat. Rev. Mol. Cell Biol.* **9**, 47-59.

Zhang, J., Yang, J., Roy, S. K., Tininini, S., Hu, J., Bromberg, J. F., Poli, V., Stark, G. R. and Kalvakolanu, D. V. (2003). The cell death regulator GRIM-19 is an inhibitor of signal transducer and activator of transcription 3. *Proc. Natl. Acad. Sci. USA* **100**, 9342-9347.

Zhang, L., Gao, L., Zhao, L., Guo, B., Ji, K., Tian, Y., Wang, J., Yu, H., Hu, J., Kalvakolanu, D. V. et al. (2007). Intratumoral delivery and suppression of prostate tumor growth by attenuated Salmonella enterica serovar typhimurium carrying plasmid-based small interfering RNAs. *Cancer Res.* **67**, 5859-5864..